

## Curcumin incorporated titanium dioxide nanoparticles as MRI contrasting agent for early diagnosis of atherosclerosis- rat model

Sainulabdeen Sherin<sup>a</sup>, Sreedharan Balachandran<sup>b</sup>, Annie Abraham<sup>\*,a</sup>

<sup>a</sup> Department of Biochemistry, University of Kerala, Kariavattom, Thiruvananthapuram 695581, India

<sup>b</sup> Department of Chemistry, M G College, Thiruvananthapuram, India

### ARTICLE INFO

#### Keywords:

Atherosclerosis  
Curcumin  
Titanium dioxide  
MRI  
Macrophage

### ABSTRACT

MRI is an excellent diagnostic technique for atherosclerosis in a non-invasive manner. Application of contrasting agents can improve its contrast through ionic properties. Macrophages and foam cells produce MCP-1 antibody, the sign of development of atherosclerosis. The work aims to develop novel curcumin incorporated titanium dioxide nanoparticles (CTNPs) conjugated with MCP-1 antibody with the specific targeting capability to macrophage-foam cells as contrasting agent for MRI. *In vivo* toxicity studies of Curcumin, TNPs and CTNPs were also done in *Sprague dawley* rats by GGT and ALP assays and found to be normal in comparison with control. Histopathology of aorta confirmed that the compound could not elicit a toxic effect in the target organ. Rats were fed with a high cholesterol diet to develop atherosclerotic foam cells and confirmed by Sudan IV staining and serum cholesterol level. CTNP-MCP-1 was injected into animals through tail vein and MRI scanning was done, gave contrasting images of atherosclerotic aorta in comparison with normal. Thus CTNPs can be used as a cost-effective contrasting tool for diagnosis of atherosclerosis at early stages in view of clinical imaging.

### Introduction

Atherosclerosis is the major disease that causes mortality and morbidity in the world, primarily. The foam cells developed from macrophages play a pivotal role in the origin and progression of atherosclerotic lesions. Over accumulation of oxidized LDL, low cholesterol efflux and increased uptake trigger the formation of foam cells (Collot-Teixeira, Martin, McDermott-Roe, Poston, & McGregor, 2007). Diagnostic tools that can directly evaluate the biochemical properties of atherosclerosis would be essential in the current scenario. MRI is currently one of the most powerful non-invasive diagnosis tools in medical science for studying the anatomy and functions of the tissues. Which offers better temporal and spatial resolution, radiationless and long effective images. It has been widely using for the diagnosis of the central nervous system, assessing cardiac function, cancer tissues etc. (Brown & Semelka, 2003). MRI is working under the principle of nuclear magnetic resonance spectroscopy. The images are generated using magnetic signals coming from the nuclei of the object to be imaged (Mansson & Bjornerud, 2001). MRI contrast agents improve the contrast

of the tissues in which they are more concentrated than other parts through the acceleration of water proton relaxation in those regions. The high sensitivity of the contrasting agent will give high contrast at a low dose. Which reduces the toxic effect of the compounds in the body. Nanomaterials can be suitable for this due to the above-said properties (Estelrich, Sánchez-Martín, & Busquets, 2015). Reports are available for specific targeting of contrasting agents using molecular markers in disease diagnosis such as inflammation, atherosclerosis, angiogenesis, apoptosis and tumors (Bogdanov, Lewin, & Weissleder, 1999). In this study, we report Curcumin incorporated titanium dioxide nanoparticles (CTNPs) as a nontoxic contrasting agent for the detection of atherosclerosis in the early development stage using the MCP-1 antibody.

Curcumin is an organic molecule isolated from *Curcuma longa*, has shown a wide range of medicinal properties in various clinical study reports (Magro et al., 2014). Even though, Curcumin shows low solubility, low absorption, rapid metabolism and reduced bioavailability, which limits its clinical efficacy (Jovanovic, Steenken, Boone, & Simic, 1999). Hence an efficient drug delivery system with improved solubility and stability will be beneficial for the successful application of

**Abbreviations:** CTNPs, Curcumin incorporated Titanium dioxide Nanoparticles; TNPs, Titanium dioxide Nanoparticle; MCP-1, Monocyte Chemoattractant Protein1; MRI, Magnetic Resonance Imaging; FTIR, Fourier Transform Infrared Spectroscopy; XRD, X-ray Diffraction Spectroscopy; DLS, Dynamic Light Scattering; SEM, Scanning Electron Microscope; EDAX, Energy Dispersive Spectroscopy; TC, Total Cholesterol; TG, triglycerides; HDL, High Density Lipoproteins; ALP, Alkaline Phosphatase; GGT, Gamma Glutamyl Transpeptidase

\* Corresponding author.

E-mail address: [annieab2013@gmail.com](mailto:annieab2013@gmail.com) (A. Abraham).

<https://doi.org/10.1016/j.vas.2020.100090>

Received 22 August 2019; Received in revised form 5 December 2019; Accepted 6 January 2020

Available online 12 May 2020

2451-943X/ © 2020 Published by Elsevier Ltd. This is an open access article under the CC BY-NC-ND license

(<http://creativecommons.org/licenses/by-nc-nd/4.0/>).

Curcumin. Reports say that poly (lactic-co-glycolic acid) nanoparticles were developed for curcumin delivery to enhance its bioavailability and intracellular transport was successful (Tiwari et al., 2013). Titanium dioxide (TiO<sub>2</sub>) is a semiconductor nanoparticle, widely using an ingredient in paints, food coloring, cosmetics, and toothpaste. It has a wide range of diagnostic and therapeutic applications due to its nontoxic nature and high chemical stability in the biological system (Yin, Wu, Yang, & Su, 2013). They are biocompatible with less or no toxicity *in vitro* and *in vivo*. Reports confirmed the reducing toxic effects when functionalized with other nontoxic molecules. The versatility of TNPs and its easily tunable physico-chemical nature is useful in the field of specific targeting.

MCP-1 is a chemoattractant protein synthesized by monocyte and endothelial cells in relation with increased production of Oxidized LDL (Yu, Fu, Zhang, Yin, & Tang, 2013) which leads to adhesion of monocyte (Cushing et al., 1990b), which induce macrophage accumulation to the vessel wall, promoting progression of atherosclerosis by producing and releasing various cytokines, chemokines, and growth factors (Luscinskas et al., 2000). The report says that Oxidized LDL has been shown to up-regulate the expression of MCP-1 *in vitro* (Ross, 1999). MCP-1 is highly expressed in macrophage-rich areas of atherosclerotic lesions in both experimental animals and humans (Cushing et al., 1990a). MCP-1 is robustly expressed in atherosclerotic lesions, suggests that MCP-1 expression could play a key role in recruiting monocytes/macrophages into early atherosclerotic lesions (Ylä-Herttuala et al., 1991). Hence, MCP-1 could be an important marker protein for early diagnosis of atherosclerosis. The present study proposes the development of a diagnostic tool conjugated with MCP-1 with improved ionic property to enhance MRI scanning image for early atherosclerosis with nontoxic nature and better biodistribution properties.

## Materials and methods

Curcumin was purchased from Sigma-Aldrich co, St. Louis and incorporated into TNPs prepared from titanium isopropoxide (Sigma Aldrich). MCP-1 antibody was purchased from Sigma Aldrich. ALP and GGT kits for *in vivo* toxicity was purchased from ERBA. MRI was done using the MRI unit Echalon Hitachi, SUT Royal Hospital Trivandrum, India. All other chemicals and solvents used were purchased from SRL, Ranbaxy and Merck, India.

### Preparation of CTNPs

#### Synthesis and characterization nanomaterials

Titanium dioxide nanoparticles and curcumin incorporated titanium dioxide nanomaterials were synthesized by reported methods with slight modification (Sawant & Kupwade, 2015). The characterization was done by using U/V Visible spectrometry, FTIR, XRD, DLS, SEM and EDAX. The stability of the compound was analyzed *in vitro* and *in vivo* models and found to be promising when compared with native Curcumin at different time intervals. These data were published with chemico-biological interactions (Sherin et al., 2017).

### Antibody conjugation

Antibody conjugation was done by using reported methods of Kanehira et al. with slight modification. The CTNPs were the first surface modified by EDC-NHS coupling (Jiang et al., 2004). CTNPs were suspended in MES buffer (1 mL, 500 mM, pH 7.4) followed by addition of NHS (2.3 mL 50 mg/mL) and EDC (1.3 mL, 10 mg/mL) at room temperature and incubated for 30 min. This was centrifuged and washed in MES buffer. The particles were resuspended in the MCP-1 antibody (10 µg/mL) and stirred at 150 rpm for 1 h. The antibody-conjugated CTNPs were centrifuged and washed in MES buffer (Rammohan et al., 2015).

## Animals experiments

*Sprague dawley* rats were obtained from the Department of Biochemistry, University of Kerala, with a bodyweight of 150–200 g. All ethical guidelines were followed for the conduct of animal experiments in strict compliance with the Institutional Animal Ethical Committee and Committee for the Purpose of Control and Supervision of Experiments on Animals (CPCSEA) Government of India, as per sanction order IAEC KU 3–2014–15 BC AA 40 (Ext) and ARRIVE guidelines.

### *In vivo* toxicity studies

Animals were grouped into four and the dosage of Curcumin, TNPs and CTNPs are given below.

Group I- Normal, Group IIa-Curcumin-1 mg/Kg Bodyweight, Group IIb-Curcumin-20/Kg Body weight, Group IIIa-TNPs – 1 mg/Kg Bodyweight, Group IIIb-TNPs-5 mg/Kg Bodyweight, Group Iva- CTNPS – 1 mg/Kg Bodyweight, Groups IVb- CTNPS – 10 mg/Kg Bodyweight

### Toxicity markers

The toxicity parameters ALP and GGT were assayed at 24 h after the administration of the nanoparticle, as described in the ERBA kit. The enzyme activity was assayed for both groups and compared with the control treatment.

### Morphological studies on red blood cell (RBC) in whole blood

The morphological alteration study on RBC was done as per the standardized method (He et al., 2009) with slight modification. Blood was collected from a rat after administration of Curcumin, TNPs and CTNPs. RBC morphology was examined by invert microscopy using wet mounted slides at 20X magnification using an inverted phase-contrast microscope Carl ZEISS Germany and captured using Jenoptic digital camera. The highest concentration is taken for photographs.

### Histopathology

Rats were anesthetized with diethyl ether and sacrificed. Aorta was removed and fixed overnight using a 10% formalin. The tissues were preserved in 70% ethanol after washing and dehydrated in ascending grades of ethanol. The xylene solution was used for cleaning and embedded in paraffin wax. The tissue blocks were sectioned in microtome at 5micrometer thickness and fixed in glass slides. The slides were stained with Mayer's hematoxylin and eosin Bancroft & Gamble, (2008). Slides were visualized using Carl ZEISS Germany and captured using Jenoptic digital camera.

### Development of atherosclerotic model

*Sprague dawley* rats were grouped into two as follows and the duration of the study was 60 days (Katsuki et al., 2014).

**Group I** - Control (normal laboratory diet)

**Group II** - Cholesterol diet (normal laboratory diet + 1% cholesterol + 0.5% cholic acid)

The development of atherosclerosis was analyzed by evaluating serum lipid profile and Sudan IV staining protocol.

Serum total cholesterol (TC), triglycerides and HDL-C concentrations were estimated using a diagnostic kit available from Agappe Diagnostics Pvt Ltd. India, according to the manufacturer's instructions. The concentration of serum LDL-C was calculated by using the Friedewalds formulae (Friedewald, Levy, & Fredrickson, 1972).

$$\text{LDL-C} = \text{TC} - (\text{HDL-C} + \text{Triglycerides}/5)$$

$$\text{Atherogenic index} = (\text{TC} - \text{HDL-C}) / \text{HDL-C}$$

At the end of experimental period, the animals were killed; the aortic arch and thoracic aorta were removed and attained for fat deposits. Briefly, the aortic arch and thoracic aorta were collected, trimmed of adhering fat, slit open and immersed in 10% formalin for

6 h. They were rinsed thoroughly for 30 min in running water and immersed in Sudan IV solution (1% in 70% isopropyl alcohol). The aortic area with fat deposition stained bright red (Tangirala, Rubin, & Palinski, 1995).

#### *Biodistribution, in vitro and in vivo toxicity studies of CTNPs, TNPs and curcumin*

The biodistribution of the compound at different tissue sites- liver, kidney, heart, spleen, aorta, lungs and serum- was assessed using the fluorescent nature of the compound at different time intervals (1, 3, 6, 12, 24, 48 h) and showed better distribution properties. The nontoxic nature of the material was studied in *in vitro* system. The data were published (Sherin et al., 2017).

#### *Biodistribution of CTNPs and MCP-1 conjugated CTNPs*

- Group I: CTNPs (20 mg/Kg body weight)
- Group II: CTNPs-MCP1 conjugate (20 mg/Kg body weight)

After injection, the animals were sacrificed at different intervals of time (1, 3, 6, 12 and 24 h post-injection). Aorta was collected for bio-distribution study by the method described by Mohanty et al. with some modifications and results were expressed in the whole aorta basis (Mohanty & Sahoo, 2010).

*Magnetic resonance imaging (MRI) in normal and atherosclerotic rats*  
Animals were grouped into two as follows. After 60 days, the GII rats (atherosclerotic) were subdivided into three groups for MRI studies,

- GII (a) - Atherosclerotic
- GII (b) - Atherosclerotic injected with CTNPs (20 mg/Kg body weight)
- GII (c) - Atherosclerotic injected with CTNP-MCP-1 Ab (20 mg/Kg body weight)

MRI was performed on Hitachi Echelon, 1.5 Tesla. The head coil is used because of the small size of the animal using the reported procedure with modification (Xu et al., 2012). Imaging was performed on three groups of animals. The samples were injected through the tail vein after anesthetized using ketamin- xylozin mixture in the ratio, 80–100 mg/kg: 5–10 mg/kg. MRI images of whole animal focusing aorta alone were taken.

## Results and discussion

### *Synthesis and characterization nanomaterials*

Synthesize and characterization of Curcumin incorporated titaniumdioxide nanoparticles were done and data were published with Chemicobiological interactions (Sherin et al., 2017). The average size of the particle was found to be 29.5 nm. Characterization results were attached as supporting data.

### *In Vivo Studies*

#### *Toxicity markers*

GGT and ALP are important toxicity markers; elevated levels of these two enzymes give an idea about the toxic nature of the compound. GGT is a marker of CVS, heart failure and all-cause mortality. Moderately elevated GGT predicted the incidence risk factors, like obesity, prehypertension, and insulin resistance. There is no indication of such abnormality in the sample treated group in comparison with the control group (Fig. 1B & C). This indicates the nontoxic nature of the compound. Previous results also ascertain our values [(Sherin et al., 2017) & (Elgrabli et al., 2015)].

#### *RBC morphology*

The interaction of samples with the circulatory system was measured by treating with RBC. RBC morphology was found to be normal after the administration of the compound (Fig. 1A). The nanoconjugates of Curcumin also showed nontoxic nature when treated with RBC (Sindhu, Rajaram, Sreeram, & Rajaram, 2014).

#### *Histopathology of aorta*

Histopathological evaluation of internal organs is complementary evidence to the biochemical analysis. Inflammation, anemia and cellular damage by nanoparticle treatment can be predicted histopathology (Li et al., 2013). Here aortic histology was done because of the target tissue. The aorta (Fig. 1F) showed normal architecture with the presence of normal aortic walls and layers. Lie et al. reported the protective role Curcumin against toxicity (Soliman, Nassan, & Ismail, 2014). Same way, reports state that TNPs administration could not elicit toxic changes in the histopathology of the rat. Our results are comparable with the previous reports (Sulaiman et al., 2015).

#### *Serum lipid profile and Sudan IV staining*

The serum lipid profile was analyzed to confirm the foam cell formation in the cholesterol-fed rats. The high fat-fed group showed high total cholesterol (LDL and TG) and low HDL cholesterol (Table 2). Cholesterol feeding in rabbits caused a significant increase in the total circulating cholesterol, LDL-cholesterol, TG, and decreases in HDL cholesterol (Tangirala et al., 1995). Sudan IV staining is used to determine the extent of atherosclerosis affecting the intimal surface throughout the entire aorta (Tangirala et al., 1995). This method provides qualitatively distinct estimates of lesion area in orthogonal axes. The result of Sudan IV staining revealed that there is a high content of plaque in the aorta of Group II in comparison with normal (Fig. 1D), which confirms the formation of atherosclerotic foam cells in the aortic area (Katsuki et al., 2014).

#### *Antibody conjugation*

MCP-1 antibody was conjugated with CTNPs and its characterization was done using Zeta potential. The Zeta potential was changed due to the presence of MCP-1 (Table 1). Reports were available for similar studies using anti-human serum albumin HSA antibody (Ab) conjugation to the surface of the TiO<sub>2</sub>/PAA nanoparticles (Kanehira et al., 2008). The nanoparticle binding increases the affinity constant of the antibody and acts as a multivalent antibody, which improves its interaction property with antigen (Cloutier et al., 2000). TiO<sub>2</sub> nanoparticles were used for such applications in cancer therapeutics with antibody recognition properties (Cai, Kubota, & Fujishima, 2003; Sakai et al., 1994; Kubota et al., 1994).

#### *Biodistribution of CTNPs and MCP-1 conjugated CTNPs*

The biodistribution of CTNPs and CTNP-MCP1 conjugate were evaluated and curcumin concentration was expressed in whole organ basis in the aortic region of atherosclerotic rats. Our previous results confirmed the stability of the Curcumin with improved bioavailability when incorporated with titanium dioxide nanoparticles (Sherin et al., 2017). Here also the graph showed a same pattern of release at tested time periods (Fig. 1D). The aortic concentration of CTNP-MCP1 conjugate was quite high in comparison with CTNPs alone. The presence of MCP1 drives CTNPs to atherosclerotic foam cells. Maximum concentration of 210 µg/organ at 3H. After one day, it has been found to be very low, which indicates its elimination from the body. The interaction of nanoparticles with several antibodies using the OH group makes it a multivalent antibody system, which improves its biodistribution at

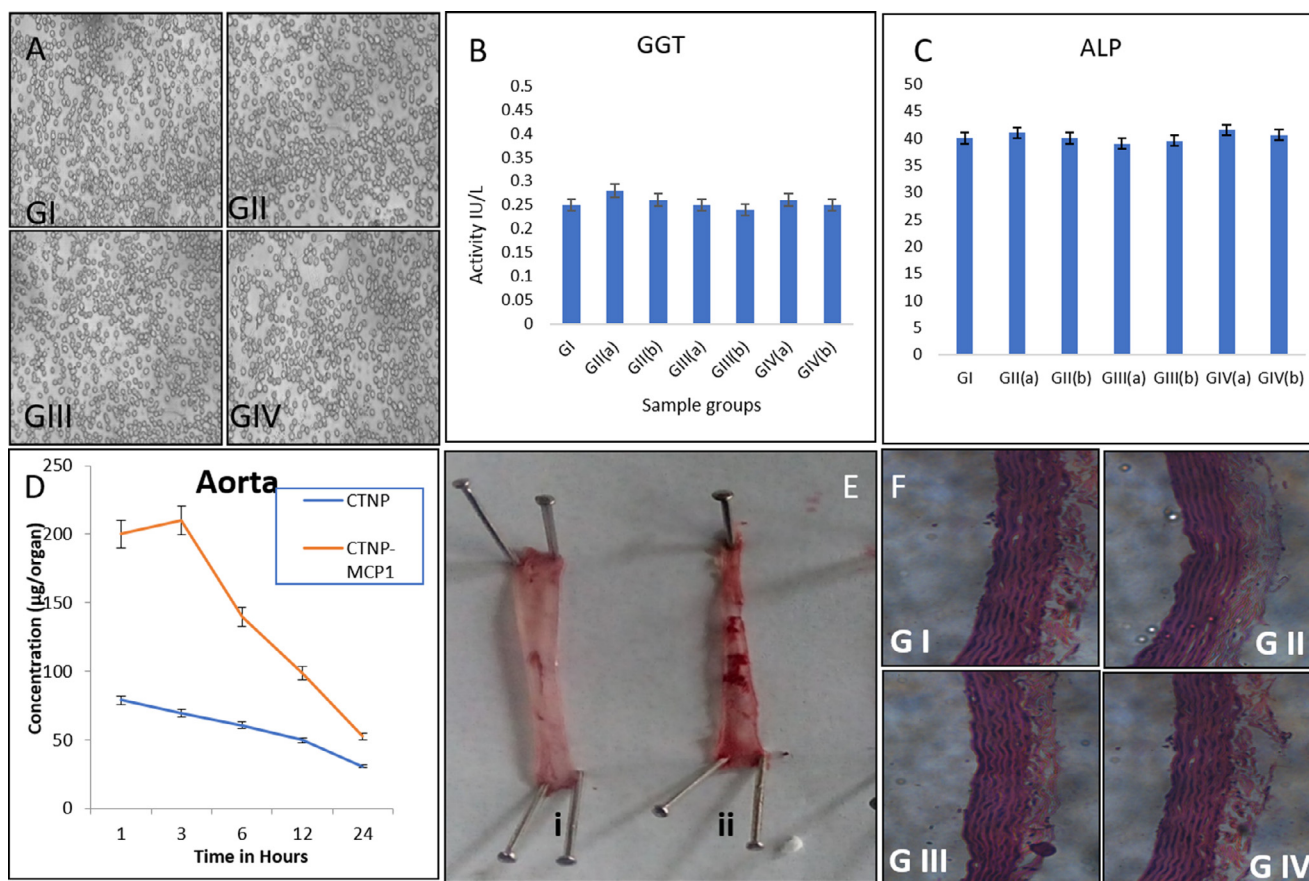


Fig. 1. (A)RBC morphology, (B) GGT assay (C) ALP assay (D) biodistribution of CTNP-MCP1 Conjugates (E) SudanIV staining of Aorta of normal (i) and cholesterol fed rat (ii) (F) Histopathology of Aorta.

specific site (Cloutier et al., 2000). Moreover, the slow release of Curcumin incorporated with TNPs improved its half-life and biodistribution (Mohanty & Sahoo, 2010). The CTNP form of Curcumin is protected from hydrolysis and conjugation, as the reports say the instability of Curcumin is due to these reactions (Anand, Sundaram, Jhurani, Kunnumakkara, & Aggarwal, 2008; Aggarwal, Kumar, & Bharti, 2003, 2007; Ma et al., 2008).

*Magnetic resonance imaging*

**Image analysis**

The 2D images (Fig: 2A & B) were reconstructed using Aquarius free viewer software. Image quality was adequate and clear enough to confirm the changes. The MRI images of a rat injected with CTNP-MCP-1 conjugates showed improved contrast at aortic regions of atherosclerotic rats, whereas normal rats showed low contrast in the aortic region and atherosclerotic rats injected with CTNPs alone showed an

unclear pattern of contrast. Once injected, the nanoparticles were accumulated in the tissue sites depending on their tissue distribution properties. The MCP-1Ag expression in the aortic region drives anti-MCP-1 conjugated CTNPs into the sites. Our biodistribution also studies the assertion of the presence of CTNP-MCP1 in the aortic area of atherosclerotic rats. The molecules accumulated in the aorta gave contrasting properties to the tissues by reducing relaxation time.

Most of the reports say that the contrasting efficiency of metal ions with the unpaired electron is mainly due to their paramagnetic properties (Koenig & Brown, 1990; Banci, Bertini, & Luchinat, 1991). The paramagnetic property of titanium dioxide in combination with carbon compounds is reported, which helps to improve its magnetic property, essential for MRI contrast (Minnekhanov, Deygen, Konstantinova, Vorontsov, & Kashkarov, 2012). Curcumin, the Carbon moiety may improve the paramagnetic property of the material. The mechanism behind the improvement of contrasting property is reducing longitudinal (T1) and transverse (T2) relaxation times of the water protons.

**Table 1**  
Zeta potential of CTNPs and CTNP-MCP-1 Ab.

Sample	Counts	Zeta potential	Counts	Particle size
CTNPs	401948.585	-55.798mV	1489	28.5nm
CTNP-MCP1	399875.867	-48.847mV	1838	39.5nm

**Table 2**  
Lipid profile of normal and atherosclerotic rat.

Sample	TC(mg/dl)	HDL C (mg/dl)	LDL C (mg/dl)	AI
Control rats	60.76±1.8	25.75±.978	35.01±1.535	1.35±0.068
Cholesterol fed	108.12±2.78	16.8±0.98	91.32±1.87	6.43±0.857

Curcumin-polymeric acid-based contrasting agents for the detection of plaques in Alzheimer's disease were reported (Patil et al., 2015). Another report confirmed the development of curcumin-conjugated nanoparticles for detecting amyloid plaques in Alzheimer's disease mice using MRI (Cheng et al., 2015). The long blood half-life of the molecule gives high relaxivity for better contrasting properties (Preda et al., 2004). Our previous results of biodistribution confirm the same (Sherin et al., 2017). Reports are available for a contrasting agent with specific targeting moieties for MRI purposes in cancer imaging (Sipkins et al., 1998; Winter et al., 2003). Altogether, considering the above results, we can conclude that the CTNP-MCP1 is a safe contrasting agent for early diagnosis of atherosclerosis by MRI.

**Conclusion**

CTNPs were used to explore the nontoxic nature of the compound using *Sprague dawley* rats. Atherosclerotic rat models were developed by a high cholesterol diet and confirmed using serum lipid profile and Sudan IV staining of the aorta. The MRI scan was done in

atherosclerotic rats after the tail vein injection of CTNPs and CTNPs-MCP-1 conjugated forms. High contrast images of the atherosclerotic aortic region when injected with CTNP-MCP-1 was visualized in comparison with normal rats. Thus the study reveals that the CTNP-MCP-1 is a nontoxic, cost-effective and bioavailable contrasting agent for a non-invasive method for early diagnosis of atherosclerosis in view of clinical imaging.

**Declaration of Competing Interest**

The authors declare that there are no conflicts of interest among them.

**Acknowledgments**

The authors were greatly thankful to Dr. Bharath Chandran (Cardiologist) and Mr. Shinu P (MRI Technician) of Patton Royal Hospital, Trivandrum, India for MRI imaging study.

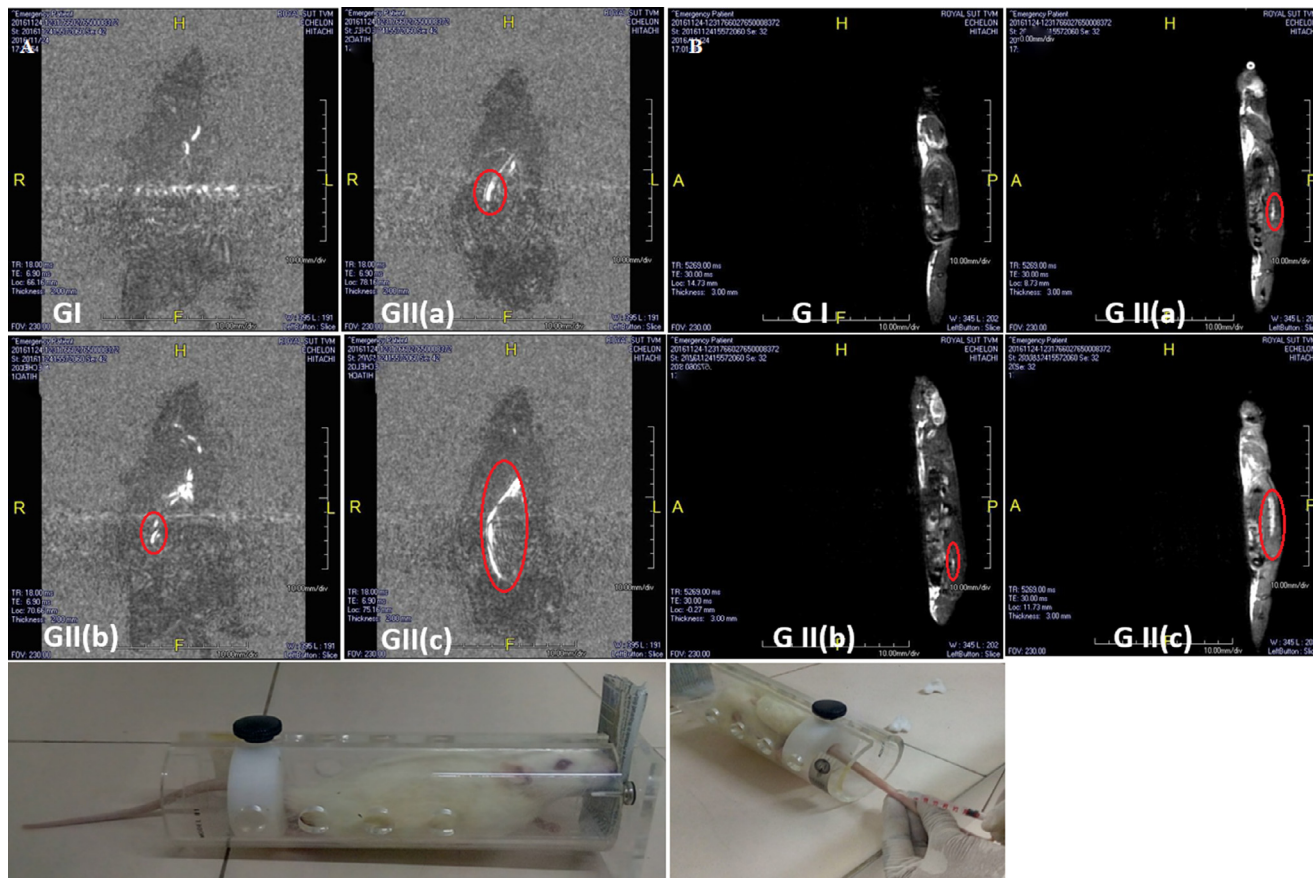


**Fig. 2.** (A) MRI Images (Dorsal view) of GI-Normal rat, GII -High cholesterol fed rat, GIII- High cholesterol fed rat injected with CTNPs, GIV- High cholesterol fed rat injected with CTNP-MCP-1 Ab. Red circle indicates aortic region. (B) MRI Images (Side view) of GI-Normal rat, GII-High cholesterol fed rat, GIII-High cholesterol fed rat injected with CTNPs, GIV- High cholesterol fed rat injected with CTNP-MCP-1 Ab. Red circle indicates aortic region.

## References

- Aggarwal, B. B., Kumar, A., & Bharti, A. C. (2003). Anticancer potential of Curcumin: Preclinical and clinical studies. *Anticancer Research*, 23(1/A), 363–398.
- Anand, P., Kunnumakkara, A. B., Newman, R. A., & Aggarwal, B. B. (2007). Bioavailability of Curcumin: Problems and promises. *Molecular Pharmacology*, 4(6), 807–818.
- Anand, P., Sundaram, C., Jhurani, S., Kunnumakkara, A. B., & Aggarwal, B. B. (2008). Curcumin and cancer: An “old-age” disease with an “age-old” solution. *Cancer letters*, 267(1), 133–164.
- Banci, L., Bertini, I., & Luchinat, C. (1991). *Nuclear and electron relaxation: The magnetic nucleus-unpaired electron coupling in solution*. Wiley-VCH.
- Bancroft, J. D., & Gamble, M. (2008). *Theory and practice of histological techniques*. Philadelphia: Churchill Livingstone Elsevier 126–127 6th edition.
- Bogdanov, A. A., Jr, Lewin, M., & Weissleder, R. (1999). Approaches and agents for imaging the vascular system. *Advanced Drug Delivery Reviews*, 37(1–3), 279–293.
- Brown, M. A., & Semelka, R. C. (2003). *MRI: Basic principles and applications* (Fifth ed.). New York: Wiley-Liss.
- Cai, R., Kubota, Y., & Fujishima, A. (2003). Effect of copper ions on the formation of hydrogen peroxide from photocatalytic titanium dioxide particles. *Journal of Catalysis*, 219(1), 214–218.
- Cheng, K. K., Chan, P. S., Fan, S., Kwan, S. M., Yeung, K. L., Wang, Y. X. J., et al. (2015). Curcumin-conjugated magnetic nanoparticles for detecting amyloid plaques in Alzheimer's disease mice using magnetic resonance imaging (MRI). *Biomaterials*, 44, 155–172.
- Cloutier, S. M., Couty, S., Terskikh, A., Marguerat, L., Crivelli, V., Pugnieres, M., et al. (2000). Streptavidin, a high avidity molecule made by tetramerization of *in vivo* biotinylated, phage display-selected scFv fragments on streptavidin. *Molecular Immunology*, 37(17), 1067–1077.
- Collet-Teixeira, S., Martin, J., McDermott-Roe, C., Poston, R., & McGregor, J. L. (2007). CD36 and macrophages in atherosclerosis. *Cardiovascular Research*, 75(3), 468–477.
- Cushing, S. D., Berliner, J. A., Valente, A. J., Territo, M. C., Navab, M., Parhami, F., et al. (1990a). Minimally modified low density lipoprotein induces monocyte chemotactic protein 1 in human endothelial cells and smooth muscle cells. *Proceedings of the National Academy of Sciences*, 87(13), 5134–5138.
- Cushing, S. D., Berliner, J. A., Valente, A. J., Territo, M. C., Navab, M., Parhami, F., et al. (1990b). Minimally modified low density lipoprotein induces monocyte chemotactic protein 1 in human endothelial cells and smooth muscle cells. *Proceedings of the National Academy of Sciences*, 87(13), 5134–5138.
- Elgrabli, D., Beaudouin, R., Jbilou, N., Floriani, M., Pery, A., Rogerieux, F., et al. (2015). Biodistribution and clearance of TiO<sub>2</sub> nanoparticles in rats after intravenous injection. *PLoS One*, 10(4), Article e0124490.
- Estelrich, J., Sánchez-Martín, M. J., & Busquets, M. A. (2015). Nanoparticles in magnetic resonance imaging: From simple to dual contrast agents. *International Journal of Nanomedicine*, 10, 1727.
- Friedewald, W. T., Levy, R. I., & Fredrickson, D. S. (1972). Estimation of the concentration of low-density lipoprotein cholesterol in plasma, without use of the preparative ultracentrifuge. *Clinical Chemistry*, 18(6), 499–502.
- He, L., Yang, L., Duan, Y., Deng, L., Sun, X., Gu, Z., et al. (2009). Cytotoxicity and hemocompatibility of a family of novel MeO-PEG-poly (D, L-lactic-co-glycolic acid)-PEG-OMe triblock copolymer nanoparticles. *Journal of Applied Polymer Science*, 113(5), 2933–2944.
- Jiang, K., Schadler, L. S., Siegel, R. W., Zhang, X., Zhang, H., & Terrones, M. (2004). Protein immobilization on carbon nanotubes via a two-step process of diimide-activated amidation. *Journal of Materials Chemistry*, 14(1), 37–39.
- Jovanovic, S. V., Steenken, S., Boone, C. W., & Simic, M. G. (1999). H-atom transfer is a preferred antioxidant mechanism of Curcumin. *Journal of the American Chemical Society*, 121(41), 9677–9681.
- Kanehira, K., Banzai, T., Ogino, C., Shimizu, N., Kubota, Y., & Sonezaki, S. (2008). Properties of TiO<sub>2</sub>-polyacrylic acid dispersions with potential for molecular recognition. *Colloids and Surfaces B: Biointerfaces*, 64(1), 10–15.
- Katsuki, S., Matoba, T., Nakashiro, S., Sato, K., Koga, J. I., Nakano, K., et al. (2014). Nanoparticle-mediated delivery of Pitavastatin inhibits atherosclerotic plaque destabilization/rupture in mice by regulating the recruitment of inflammatory monocytes. *Circulation*, 129(8), 896–906.
- Koenig, S. H., & Brown, R. D., III (1990). Field-cycling relaxometry of protein solutions and tissue: Implications for MRI. *Progress in Nuclear Magnetic Resonance Spectroscopy*, 22(6), 487–567.
- Kubota, Y., Shuin, T., Kawasaki, C., Hosaka, M., Kitamura, H., Cai, R., et al. (1994). Photokilling of T-24 human bladder cancer cells with titanium dioxide. *British journal of cancer*, 70(6), 1107–1111.
- Li, G., Chen, J. B., Wang, C., Xu, Z., Nie, H., & Qin, X. Y. (2013). Curcumin protects against acetaminophen-induced apoptosis in hepatic injury. *World Journal of Gastroenterology*, 19(42), 7440.
- Luscinskas, F. W., Gerszten, R. E., GARCIA-ZEPEDA, E. A., LIM, Y. C., Yoshida, M., & Ding, H. A. (2000). C-C and C-X-C Chemokines trigger firm adhesion of monocytes to vascular endothelium under flow conditions. *Annals of the New York Academy of Sciences*, 902(1), 288–293.
- Ma, Z., Haddadi, A., Molavi, O., Lavasanifar, A., Lai, R., & Samuel, J. (2008). Micelles of poly (ethylene oxide)-b-poly (ε-caprolactone) as vehicles for the solubilization, stabilization, and controlled delivery of Curcumin. *Journal of Biomedical Materials Research Part A: An Official Journal of The Society for Biomaterials, The Japanese Society for Biomaterials, and The Australian Society for Biomaterials and the Korean Society for Biomaterials*, 86(2), 300–310.
- Magro, M., Campos, R., Baratella, D., Lima, G., Holá, K., Divoky, C., et al. (2014). A magnetically drivable nanovehicle for Curcumin with antioxidant capacity and MRI relaxation properties. *Chemistry—A European Journal*, 20(37), 11913–11920.
- Mansson, S., & Björnerud, A. (2001). *Physical principles of medical imaging by nuclear magnetic resonance. The chemistry of contrast agents in medical magnetic resonance imaging*. Chichester: John Wiley and Sons, Ltd 1–43.
- Minnekhanov, A. A., Deygen, D. M., Konstantinova, E. A., Vorontsov, A. S., & Kashkarov, P. K. (2012). Paramagnetic properties of carbon-doped titanium dioxide. *Nanoscale Research Letters*, 7(1), 333.
- Mohanty, C., & Sahoo, S. K. (2010). The *in vitro* stability and *in vivo* pharmacokinetics of Curcumin prepared as an aqueous nanoparticulate formulation. *Biomaterials*, 31(25), 6597–6611.
- Patil, R., Gangalum, P. R., Wagner, S., Portilla-Arias, J., Ding, H., Rekechenetskiy, A., et al. (2015). Curcumin targeted, polymeric acid-based MRI contrast agent for the detection of Aβ plaques in Alzheimer's disease. *Macromolecular Bioscience*, 15(9), 1212–1217.
- Preda, A., Novikov, V., Möglicher, M., Turetschek, K., Shames, D. M., & Brasch, R. C. (2004). MRI monitoring of Avastin™ antiangiogenesis therapy using B22956/1, a new blood pool contrast agent, in an experimental model of human cancer. *Journal of Magnetic Resonance Imaging: An Official Journal of the International Society for Magnetic Resonance in Medicine*, 20(5), 865–873.
- Rammohan, A., Mishra, G., Mahaling, B., Tayal, L., Mukhopadhyay, A., Gambhir, S., et al. (2015). PEGylated carbon nanocapsule: A universal reactor and carrier for *in vivo* delivery of hydrophobic and hydrophilic nanoparticles. *ACS Applied Materials & Interfaces*, 8(1), 350–362.
- Ross, R. (1999). Atherosclerosis—An inflammatory disease. *The New England Journal of Medicine*, 340, 115–126 Find this article online.
- Sakai, H., Ito, E., Cai, R. X., Yoshioka, T., Kubota, Y., Hashimoto, K., et al. (1994). Intracellular Ca<sup>2+</sup> concentration change of T24 cell under irradiation in the presence of TiO<sub>2</sub> ultrafine particles. *Biochimica et Biophysica Acta (BBA)—General Subjects*, 1201(2), 259–265.
- Sawant, V. J., & Kupwade, R. V. (2015). Functionalization of TiO<sub>2</sub> nanoparticles and curcumin loading for enhancement of biological activity. *Der Pharmacia Lettre*, 7, 37–44.
- Sherin, S., Sheeja, S., Devi, R. S., Balachandran, S., Soumya, R. S., & Abraham, A. (2017). *In vitro* and *in vivo* pharmacokinetics and toxicity evaluation of Curcumin incorporated titanium dioxide nanoparticles for biomedical applications. *Chemico-Biological Interactions*, 275, 35–46.
- Sindhu, K., Rajaram, A., Sreeram, K. J., & Rajaram, R. (2014). Curcumin conjugated gold nanoparticle synthesis and its biocompatibility. *Rsc Advances*, 4(4), 1808–1818.
- Sipkins, D. A., Cheresch, D. A., Kazemi, M. R., Nevin, L. M., Bednarski, M. D., & Li, K. C. (1998). Detection of tumor angiogenesis *in vivo* by a  $\alpha$  v  $\beta$  3-targeted magnetic resonance imaging. *Nature medicine*, 4(5), 623.
- Soliman, M. M., Nassan, M. A., & Ismail, T. A. (2014). Immunohistochemical and molecular study on the protective effect of Curcumin against hepatic toxicity induced by paracetamol in Wistar rats. *BMC Complementary and Alternative Medicine*, 14(1), 457.
- Sulaiman, F. A., Akanji, M. A., Oloyede, H. O. B., Sulaiman, A. A., Olatunde, A., & Joel, E. B. (2015). Oral exposure to silver/gold nanoparticles: Status of rat lipid profile, serum metabolites and tissue morphology. *Journal of Medical Sciences*, 15(2), 71.
- Tangirala, R. K., Rubin, E. M., & Palinski, W. (1995). Quantitation of atherosclerosis in murine models: Correlation between lesions in the aortic origin and in the entire aorta, and differences in the extent of lesions between sexes in LDL receptor-deficient and apolipoprotein E-deficient mice. *Journal of Lipid Research*, 36(11), 2320–2328.
- Tiwari, S. K., Agarwal, S., Seth, B., Yadav, A., Nair, S., Bhatnagar, P., et al. (2013). Curcumin-loaded nanoparticles potentially induce adult neurogenesis and reverse cognitive deficits in Alzheimer's disease model via canonical Wnt/ $\beta$ -catenin pathway. *ACS Nano*, 8(1), 76–103.
- Winter, P. M., Caruthers, S. D., Kassner, A., Harris, T. D., Chinen, L. K., & Allen, J. S. (2003). Molecular imaging of angiogenesis in nascent Vx-2 rabbit tumors using a novel  $\alpha$ v $\beta$ 3-targeted nanoparticle and 1.5 T magnetic resonance imaging. *Cancer Research*, 63(18), 5838–5843.
- Xu, W., Kattel, K., Park, J. Y., Chang, Y., Kim, T. J., & Lee, G. H. (2012). Paramagnetic nanoparticle T 1 and T 2 MRI contrast agents. *Physical Chemistry Chemical Physics*, 14(37), 12687–12700.
- Yin, Z. F., Wu, L., Yang, H. G., & Su, Y. H. (2013). Recent progress in biomedical applications of titanium dioxide. *Physical Chemistry Chemical Physics*, 15(14), 4844–4858.
- Ylä-Herttuala, S., Lipton, B. A., Rosenfeld, M. E., Särkioja, T., Yoshimura, T., & Leonard, E. J. (1991). Expression of monocyte chemoattractant protein 1 in macrophage-rich areas of human and rabbit atherosclerotic lesions. *Proceedings of the National Academy of Sciences*, 88(12), 5252–5256.
- Yu, X. H., Fu, Y. C., Zhang, D. W., Yin, K., & Tang, C. K. (2013). Foam cells in atherosclerosis. *Clinica Chimica acta*, 424, 245–252.